



HAL
open science

In-vitro liver model using microfabricated scaffolds in a modular bioreactor

Bruna Vinci, Daniela Cavallone, Giovanni Vozzi, Claudio Domenici, Maurizia Brunetto, Arti Ahluwalia

► **To cite this version:**

Bruna Vinci, Daniela Cavallone, Giovanni Vozzi, Claudio Domenici, Maurizia Brunetto, et al.. In-vitro liver model using microfabricated scaffolds in a modular bioreactor. *Biotechnology Journal*, 2009, 5 (2), pp.232. 10.1002/biot.200900074 . hal-00525500

HAL Id: hal-00525500

<https://hal.science/hal-00525500>

Submitted on 12 Oct 2010

HAL is a multi-disciplinary open access archive for the deposit and dissemination of scientific research documents, whether they are published or not. The documents may come from teaching and research institutions in France or abroad, or from public or private research centers.

L'archive ouverte pluridisciplinaire **HAL**, est destinée au dépôt et à la diffusion de documents scientifiques de niveau recherche, publiés ou non, émanant des établissements d'enseignement et de recherche français ou étrangers, des laboratoires publics ou privés.



In-vitro liver model using microfabricated scaffolds in a modular bioreactor

Journal:	<i>Biotechnology Journal</i>
Manuscript ID:	biot.200900074.R1
Wiley - Manuscript type:	Research Article
Date Submitted by the Author:	24-Jul-2009
Complete List of Authors:	Vinci, Bruna; University of Pisa, Centro Interdipartimentale di Ricerca Pisa, Cavallone, Daniela; Azienda Ospedaliera Universitaria Pisana, Epatologia Vozzi, Giovanni; University of Pisa,, Centro Interdipartimentale di Ricerca Domenici, Claudio; CNR, Institute of Clinical Physiology Brunetto, Maurizia; Azienda Ospedaliera Universitaria Pisana, Epatologia Ahluwalia, Arti; University of Pisa, Centro Interdipartimentale di Ricerca
Keywords:	Scaffold , Bioreactor, Microfabrication, Liver model



Research Article ((6328 words))

In-vitro liver model using microfabricated scaffolds in a modular bioreactor

Bruna Vinci¹, Daniela Cavallone², Giovanni Vozzi¹, Daniele Mazzei¹ Claudio Domenici³,
Maurizia Brunetto² and Arti Ahluwalia^{1*}

¹Interdepartmental Research Center “E. Piaggio”, University of Pisa, via Diotisalvi, 2, 56126 Pisa,

² U.O. Epatologia, Azienda Ospedaliera Universitaria Pisana, via Paradiso 2, Cisanello, 56124 Pisa

³ CNR Institute of Clinical Physiology, via G Moruzzi, 1 56100, Pisa

Keywords: Scaffold, microfabrication, liver model, bioreactor.

***Address for Correspondence:**

Arti Ahluwalia
Interdepartmental Research Center “E. Piaggio”,
University of Pisa, via Diotisalvi, 2,
Pisa, 56126
Italy
Fax +39 0502217051
Email: arti.ahluwalia@ing.unipi.it

Abbreviations:

PAM: Pressure Activated Microsyringe

MCmB: MultiCompartment modular Bioreactor

3D: 3 dimensional

2D: 2 dimensional

CAD/CAM: Computer Aided Design/Computer Aided Manufacturing

PLGA: poly-DL-lactide-co-glycolide

PLLA: poly-L-lactide

PDMS: Polydimethylsiloxane

EMEM: Eagle's minimal essential medium

ANCOVA: Analysis of covariance

ABSTRACT

Hepatocyte function on three-dimensional microfabricated polymer scaffolds realised with the Pressure Activated Microsyringe (PAM) was tested in static and dynamic conditions. The dynamic cell culture was obtained using the MCmB (MultiCompartment modular Bioreactor) system. Hepatocyte cell density, glucose consumption, and albumin secretion rate were measured daily over a week. Cells seeded on scaffolds showed an increase in cell density compared with monolayer controls. Moreover, in dynamic culture, cell metabolic function increased three times in comparison with static monolayer cultures. These results suggest that cell density and cell-cell interactions are mediated by the architecture of the substrate, while the **endogenous** biochemical functions are regulated by a sustainable supply of nutrients and interstitial-like flow. Thus a combination of three-dimensional scaffolds and dynamic flow conditions are both important for the development of a hepatic tissue model for applications in drug testing and regenerative medicine.

Keywords: Scaffold, microfabrication, liver model, bioreactor.

I. Introduction

A great deal of effort is being made to preserve liver specific function *in-vitro*. There are several driving forces for this, perhaps the two most important are drug testing and bioartificial liver devices. For the moment, the prevailing opinion in the literature is that it is impossible to maintain an adequately differentiated hepatic phenotype after isolation from the liver for more than a week [1]. Several parameters are known to play a role in maintaining liver function; among these are the presence of an adequate nutrient supply, an extra cellular environment rich with ligands for adhesion and signalling, and a spatial architecture resembling that of the native liver, as well as a multicomponent medium. These parameters form what we call here the tripartite of cues: a trio of biochemical, biophysical and biomechanical signalling systems which interact synergically to support both form and function in all living tissues [2].

A wide variety of methods have been and are being developed to maintain and study the function of hepatocytes *in-vitro*. Many of these are based on devising complex cocktails of culture medium, which often include inducing agents in order to drive hepatocytes towards expression of P450 cytochromes [3]. Others use engineering based methods such as scaffolds and bioreactors. Several authors have used: three dimensional (3D) structures such as collagen [4], or loofa sponges in static and perfused cell culture conditions [5] and hydrogel encapsulated hepatocytes [6]. In the past few years the use of bioreactors has become very popular because a dynamic cell culture system allows efficient metabolite exchange, and may also provide an indirect physical stimulus through percolative or interstitial-like flow [7]. The bioreactors can be divided into 2 main groups: those for large scale culture, such as flat membrane systems, and microfabricated systems which involve 2 or 3 dimensional cultures and microfluidics. The simplest systems are continuous flow reactors such as that proposed by Catapano and De Bartolo, which are useful for large scale culture, particularly for artificial liver applications [8]. A microfabricated array reactor with deep wells for hepatocyte spheroids was described by Powers *et al.* [9, 10]. In this system, the wells were perfused by the medium and the cells were reported to remain viable for 2 weeks, with high levels of urea and albumin secretion. Hongo *et al.*, and Kataoka *et al.* describe the culture of porous scaffolds in a radial flow bioreactor so combining two of the cues in a single experiment [11, 12]. It is also recognised that coculture of hepatocytes and non parenchymal cells augments liver phenotypic function. Bhatia *et al.* pioneered the use of two dimensional (2D) micro patterns in mono and co-culture, and they have reported on various combinations of heterotypic cultures as well as a comparative study which highlights the differences in gene expression in different coculture combinations [13,14]. Several reports by the group of Yarmush and Toner on microfabricated grooved substrates for hepatocyte

1
2
3 cocultures have been published, showing the advantage of grooves with respect to flat surfaces
4 [15,16]. Finally, sandwich cultures, in which hepatocytes are either supplied with an adhesive
5 protein based roof and floor to recreate a pseudo 3D extracellular matrix environment have also
6 been widely reported to enhance hepatic function [17]. Despite the extensive literature on the
7 subject, it is not clear how strongly each of these parameters influence hepatic phenotype, quite
8 likely the biochemical, biophysical and mechanical stimuli provide multiple cues which act in
9 unison to mimic the *in-vivo* hepatic environment. The aim of this work was to gain a better
10 understanding of the role of a 3D architecture and convective mass transfer on hepatocytes *in-vitro*.
11 We therefore designed an *in-vitro* model of the liver by using a bottom up engineering approach,
12 that is by a step wise increase of the number of cues in the system. For this study we considered
13 only cues which can be controlled externally using mechanical and structural design parameters.
14 Biochemical control of hepatocyte function is far more complex because the cells themselves
15 modulate the chemistry of their environment. Firstly the influence of a 3D open-pore
16 microfabricated scaffold on HepG2 cell proliferation and metabolic function was assessed using two
17 different biomaterials. The most suitable material was then selected for experiments using a low
18 shear, high flow bioreactor [18], and both cell proliferation and metabolism were analysed and
19 compared with controls.
20
21
22
23
24
25
26
27
28
29
30
31
32
33
34
35
36

37 **2 Materials and Methods**

38 **2.1 Microfabrication with PAM**

39
40 The syringe-based deposition method PAM (Pressure Assisted Microsyringe) has been described in
41 several references [19]. Basically it consists of a pressure activated syringe which is controlled by a
42 CAD/CAM (Computer Aided Design/Computer Aided Manufacturing) fabrication system. The
43 syringe is a stainless steel barrel with a glass capillary needle with a diameter of 5 to 20 μm . It is
44 filled with a viscous polymer solution and mounted on a 3 axis micropositioner. Pressurised air is
45 used to extrude the polymer solution through the micro-needle and deposit it on a solid substrate
46 such as a glass cover slip. The CAD/CAM system allows an infinite range of structures with a
47 lateral resolution of 5 μm to be designed and fabricated. 3D polymeric scaffolds are assembled by
48 depositing a water soluble polymeric spacer (Hydrofilm, Lucart, Italy) of about 10-20 μm between
49 the layers. This avoids the collapse of subsequent layers and creates large pores in which cells are
50 able to penetrate and adhere. After the microfabrication step, scaffolds are immersed in water and
51
52
53
54
55
56
57
58
59
60

1
2
3 during this process the polymer spacer is dissolved away and the scaffolds float off the substrates
4 and can be handled with tweezers.

5
6 PAM has the highest resolution of all 3D CAD/CAM microfabrication methods used in tissue
7 engineering, and the fidelity of the scaffolds is about 10% [20]. Apart from the machine dependent
8 deposition parameters such as needle bore size and motor speed and precision, the fidelity depends
9 mainly on the viscosity and surface tension of the polymer.
10
11
12

13 **2.2 Polymer and scaffold treatment**

14
15 The polymers used in this study were: PLGA, poly-DL-lactide-co-glycolide 75:25 and PLLA (poly-
16 L-lactide) (Lactel, NPPHarm-F, Bazainville, France). PLGA and PLLA are biodegradable polymers
17 widely used in tissue engineering applications. Our group has tested these polymers in the form of
18 spin-coated films and PAM scaffolds and their suitability for cell adhesion and tissue engineering
19 has been evaluated [21]. Solutions of 20% (w/v) PLGA and 10% (w/v) PLLA in chloroform
20 respectively have excellent deposition characteristics in terms of their viscosity and surface tension,
21 and these concentrations were used for all experiments. Hexagonal unit cell structures were
22 microfabricated with 50 μm line width and 500 μm unit side length, (Figure 1A illustrates the
23 definition of these terms) and were composed of three layers with 70 hexagons each (Figure 1A).
24 Each layer was laterally offset by 250 μm so that the hexagons were not piled flush but formed
25 small open pores in the scaffold. The dimensions were chosen because they mimic the characteristic
26 size of hepatic lobules [22]. Figure 1B shows an example of a PLGA 3D scaffold. Polymer films
27 were realized by spin coating (Delta 10TT, SÜSS MicroTec) at 7500 rpm for 15 seconds on 13 mm
28 diameter glass cover slips. These films were used as a monolayer static control in order to
29 investigate how cell function is influenced by a 3D topology and to compare and to normalize the
30 experimental data with respect to the polymer's intrinsic characteristics rather than laboratory tissue
31 culture plastic.
32
33
34
35
36
37
38
39
40
41
42
43
44

45 Before cell seeding to remove all traces of solvent, the scaffolds and films were placed in a
46 dessicator under vacuum for at least a week, and then washed extensively with deionised water and
47 dried in an oven at 50°C. Following this, the structures were placed in 24 well plates (Sarstedt,
48 Verona, Italy) and sterilized using a standard hospital H₂O₂ Gas-Plasma protocol available at our
49 clinical facilities. In order to promote cell attachment, 5 $\mu\text{g}/\text{cm}^2$ purified collagen, PureCol™
50 (INAMED, Leimuiden, Netherlands), was pipetted over the structures and after one hour's
51 incubation at 37°C, they were washed with PBS three times and equilibrated with fresh medium
52 overnight in the incubator.
53
54
55
56
57
58
59
60

2.3 Bioreactor design and assembly

The MCmB bioreactor was developed to enable cell and tissue culture in a variety of configurations [18, 23]. Its main characteristics are high flow rates and low wall shear stresses. In its simplest form, as used in this work, it is made of PDMS (Polydimethylsiloxane, Dow Corning, Italy), and has the same dimensions as a 24- microwell plate (15 mm diameter and 2 ml volume). A patented sloping roof ensures the absence of bubbles in the chamber. A FEM (Finite Element Modeling) model of the cell culture chamber was developed in order to study the shear stress at the cell surface. Cosmos Floworks, a Solidworks™ (Dassault Systèmes SolidWorks Corp. Concord, MA, USA) extension which allows fluid-dynamic FEM analysis as well as 3D CAD was used for this purpose. In the fluid dynamic model we used the following system constants: viscosity= 10^{-3} Pa·s, fluid density = 1000 kg/m^3 , medium flow rate= $250 \text{ }\mu\text{L/min}$, pressure= 1 atmosphere or 760 mmHg, temperature= $37 \text{ }^\circ\text{C}$ and no slip boundary conditions. Figure 2A shows a three dimensional representation of the chamber, and in Figure 2B the velocity streamlines modelled using SolidWorks™ are drawn.

Three MCmB bioreactors were connected in parallel to a pump (Instec P720, Instec, Boulder, Colorado, USA) and a mixing chamber which has a volume of 2 ml and serves to facilitate assembly of the flow circuit, allows gaseous mixing, and acts as a bubble trap. A flow rate of $250 \text{ }\mu\text{L/min}$ was used in all experiments, and the average shear stress in the cell culture zone was calculated by fluid dynamic simulation. The maximum wall shear stress at the flow rate used was about 10^{-5} Pa , and .

In our experience, even small flow rates may damage hepatocytes. Therefore all the cultures were protected with a thin coating of alginate as described in the section on cell culture. In the bioreactor experiments the medium was not changed since sufficient nutrients were present in the 10 ml closed loop circuit (2 ml in each bioreactor, 7 ml in the mixing chamber and about 1 ml in the tubing).

2.4 Cell culture

Since primary hepatocytes *in-vitro* rapidly lose liver-morphology and differentiated functions, in this study we used the HepG2 cell line as an alternative model cell. HepG2 cells maintain the main synthetic and endogenous functions of primary hepatocytes, as well some exogenous metabolic functions [24]. Furthermore, the HepG2 cell line is simple to culture and by virtue of its immortality, it is possible to make standard comparisons which remain valid over time and for all experiments.

1
2
3 HepG2 human hepatoblastoma cells were a kind gift from Dr. S. Quarta, University of Padova. The
4 cells were grown in Eagle's minimal essential medium (EMEM, glucose 1g/liter) supplemented
5 with 5% fetal bovine serum, 1% non essential aminoacids, 1% EMEM vitamins, 2 mM L-
6 glutamine, 100 U/ml penicillin and 100 µg/ml streptomycin in a humidified incubator at 37°C, 5%
7 CO₂ (Hereaus SpA, Milan, Italy). The cells were all used at the same passage (# 22 after receipt)
8 and passaged using 0.05 % trypsin with 0.02% EDTA in PBS (all reagents from Eurolone, Milan,
9 Italy). 100,000 cells/cm² were seeded on the films or scaffolds using 2 ml of complete medium per
10 well. After 24 hours the structures were moved to a new microwell plate to eliminate interference
11 from non adherent cells.
12

13 Both scaffolds and films were coated with an alginate film consisting of 250 µl 1% sodium alginate
14 dissolved in serum free medium, cross linked with 50 µl of 1% CaCl₂ (both from Sigma-Aldrich,
15 Milan, Italy). Excess alginate was removed with a pipette. The resulting film had a thickness of a
16 few tens of microns as measured by an optical profilometer (Opto NCDT, model ILD1400-10, UK),
17 having a nominal resolution of 1 µm. The profilometer uses a small laser spot (0.7 mm×0.5 mm)
18 which is reflected off a surface. Displacements were calibrated using an uncoated glass slide as a
19 reference. The coating was not uniform and flat as observed by an optical microscope, and this was
20 also reflected in the scatter of the profilometer readings across the slide (40 to 100 µm). At the low
21 alginate concentrations used, the diffusion coefficient of oxygen and of small solutes is similar to
22 that in water [25, 26, and 27].
23

24 Finally 2 ml of fresh medium was added to each well to begin the experiment. Cells were
25 maintained on the structures for a week and cell counting and medium collection was performed
26 daily. The experiment was performed in triplicate using 21 structures, three samples were sacrificed
27 for counting per day, and the culture medium was changed every third day.
28

2.5 Bioreactor Culture

29 For the dynamic experiments, cells were seeded as described for the static cultures. 24 hours after
30 seeding, the scaffolds were transferred to a glass slide, placed in the MCmB (one scaffold per
31 bioreactor) and coated with an alginate film. The alginate coating was used to protect the cells from
32 direct mechanical stress, whilst allowing adequate nutrient diffusion. The coating also stops the
33 scaffolds from floating off the slides. Medium was perfused and re-circulated through the chambers
34 at a flow rate of 250 µl/min. A total of 21 scaffolds were used for the bioreactor experiments. In
35 particular, three bioreactors with three scaffolds were used per time point, and at the end of each
36 time point the bioreactors were disassembled for cell counting and a final sample of medium
37

1
2
3 collected. In addition up to 200 μl of media (50 μl per assay) was withdrawn from the mixing
4 chambers for analysis at fixed intervals. All cell culture experiments were carried out in the same
5 incubator.
6
7
8
9

10 2.6 Cell Analysis and Assays

11 Cell Viability and Density

12 At the end of each time point the cells adhered on the structures were trypsinised off the scaffolds
13 and membranes and counted using a Burker chamber. Cell viability was evaluated using trypan blue
14 exclusion, and this was always greater than 95%. To ensure that all cells had been accounted for,
15 the scaffolds were also stained with trypan blue and typically only a few cells were observed on the
16 scaffolds after trypsinization. Cell morphology was assessed using an optical microscope (AX70,
17 Olympus Italia, Milan).
18

19 Because the 3D scaffolds are composed of 3 layers of hexagons, the “true” area available for cell
20 adhesion is difficult to estimate. According to the CAD model shown in Fig 1A the total surface
21 area of one layer of the scaffold is about 0.06 cm^2 , however a 3D scaffold may also have adhesive
22 surfaces in more than one plane. Therefore we use the term “nominal area” to refer to the overall
23 area of the scaffold or film. Cell densities are expressed as the total number of cells counted divided
24 by the nominal 2D-surface area of the samples. The PAM scaffolds have a nominal surface area of
25 0.8 cm^2 and a large percentage of this is free space of the pores, while the spin-coated films have an
26 area of 1.33 cm^2 .
27
28
29
30
31
32
33
34
35
36
37
38

39 Biochemical assays

40 Albumin production, which characterizes the specific functional activity of liver cells, was
41 measured by an enzyme-linked immunosorbent assay (ELISA) (Bethyl Laboratories, Montgomery,
42 TX USA). A standard curve was made using purified human albumin under the conditions
43 recommended by the manufacturer. Species specificity of the anti-human albumin antibodies was
44 verified using fetal bovine serum. Glucose consumption and urea production were quantified using
45 commercial enzymatic kits according to the manufacturers’ instructions (Megazyme International
46 Poncarale, Italy and Urea Kit, Sigma-Aldrich, Milan, Italy respectively). In order to compare data
47 from different experiments with different cell numbers and media volumes the glucose, albumin
48 and urea data are expressed as quantities consumed or produced per cell per day, and therefore as
49 rates, not cumulative quantities.
50
51
52
53
54
55
56
57
58

59 Statistical analysis

1
2
3 Statistical analysis was performed using analysis of covariance - ANCOVA for comparison of
4 trends (Matlab Statistics Toolbox, The MathWorks Inc.); a p value of less than 0.05 was considered
5 statistically significant. Each data point is represented as the mean and standard deviation of 3
6 samples and at each time point 3 scaffolds were analyzed destructively (by trypsinization) for cell
7 counting.

14 3. Results

15 3.1 Comparison between 2D films and 3D scaffolds in static culture

16 As shown in Figure 3, the cell density was higher on the scaffolds than on films particularly from
17 day 4 onwards (ANCOVA, $p < 0.01$). The cells seeded on 3D structures proliferated throughout the
18 duration of the experiment and the rate of increase was modulated by the media changes (day 3 and
19 6), whereas the cells seeded on 2D films proliferated until the fourth day and the rate of increase did
20 not appear to be influenced by the media changes (day 3 and 6). This could be due to removal of
21 loosely adherent cells when the medium was aspirated.

22 Figure 4 shows the glucose consumption rate. Glucose was consumed at a constant rate (5.2 ± 0.3
23 $\text{ng}/(\text{cell}/\text{day})$, $p = 0.004$, ANCOVA) by cells seeded on 3D scaffolds and the consumption was not
24 influenced by the continuous cell proliferation in 3D. The cells on the 2D films consumed a higher
25 quantity of glucose than 3D scaffolds in the first two days. After this period, the glucose
26 consumption per cell was constant and similar to that of the 3D scaffolds. The initial high glucose
27 consumption by cells seeded on polymeric films does not seem to depend on the rate of
28 proliferation but could represent increased energetic requirements due to cell-matrix interactions. In
29 fact 2D films present a large surface area to the cells for adhesion whereas the 3D scaffold is more
30 porous and there are fewer adhesive sites per unit area. Once the adhesion process is over, all cells
31 converge to a constant glucose consumption rate.

32 Albumin is one of the functional marker proteins of the liver. Human albumin was produced in
33 similar quantities by 3D scaffolds and 2D films during the experiment (Figure 5), and the
34 production rates are similar to those reported in [24, 28]. An analysis of the production rates using
35 ANCOVA indicated that the albumin production rate was higher in the first two days than on
36 subsequent days (days 1 to 2: $0.82 \pm 0.32 \text{ pg}/(\text{cell}/\text{day})$, days 4 to 7: $0.49 \pm 0.05 \text{ pg}/(\text{cell}/\text{day})$, $p < 0.05$).
37 Although the cell proliferation rate was higher on the 3D scaffolds than on the 2D films, we found
38 no differences cell behaviour with respect to the two polymers. PLGA and PLLA are known to have
39 different surface and mechanical properties, and this result implies that in our experiments only the
40
41
42
43
44
45
46
47
48
49
50
51
52
53
54
55
56
57
58
59
60

1
2
3 microtopology influences cell proliferation and not the differences in physico-chemical properties
4 between the polymers.
5
6
7

8 9 **3.2 3D scaffolds in dynamic conditions in the MCmB**

10 Having established that 3D scaffolds can increase the cell density consistently for up to 7 days, the
11 next step was to select the polymer to be used. Since there were no significant cell metabolic and
12 proliferative differences between the 2 polymers, PLGA was selected for successive experiments
13 because of its deposition characteristics. The choice was based on the fact that 20% PLGA is
14 slightly more viscous than 10% PLLA, and the scaffolds obtained using the PAM system are of
15 higher fidelity than the corresponding PLLA scaffolds [29].
16
17

18 For each time point three bioreactors were set up in parallel with one 3D scaffold per chamber. In
19 the bioreactors, the cell density increased smoothly over time, as the peaks due to media changes
20 were absent, and density values were similar to those in static conditions (Figure 6).
21
22

23 Glucose consumption was slightly higher in the MCmB with a constant consumption rate of $7.6 \pm$
24 0.1 ng/(cell/ day) ($p=0.0001$ ANCOVA) with respect to the 3D scaffold in static conditions (5.2 ± 0.2
25 $\text{ng}/(\text{cell}/\text{day})$, $p=0.001$, ANCOVA) (Figure 7). Therefore the cell energy requirements are greater in
26 the bioreactor, and glucose is used as a substrate. This may be due to an upregulation of liver-
27 specific synthetic function in the bioreactor, as shown in Figure 8. A large increase in albumin
28 production rate per cell was observed in dynamic culture. In the first 2 days; the albumin production
29 rate was 10 times higher in the MCmB than in static conditions and then decreased progressively
30 maintaining a value 4~5 times greater than in static culture. In fact, the average albumin production
31 rate in the bioreactor over the 7 days was 3.12 ± 0.43 pg/(cell/day), compared with 0.65 ± 0.16
32 $\text{pg}/(\text{cell}/\text{day})$ ($p=0.02$, ANCOVA) in the scaffolds in static conditions .
33
34

35 To ensure that the increased albumin production rate was not due to the increased volume of
36 medium in the bioreactor, a final experiment was performed using 3D scaffolds cultured in 50 mm
37 Petri dishes in which the total medium volume was 10 ml. The albumin production rate was 0.50
38 ± 0.14 pg/(cell/day) over the 2 day period of analysis, indicating that the volume of medium does not
39 influence the secretion rate of this protein in static conditions.
40
41

42 Figure 9 shows the that urea production rate, indicative of an intact nitrogen metabolism pathway, is
43 significantly enhanced in the dynamic 3D culture with respect to both the 2D and 3D static
44 conditions. In static conditions, the 2D films and 3D scaffolds converged to the same production
45 rate towards the end of the culture period (136 ± 101 pg/(cell/day)), while the average urea
46 production rate in the bioreactor was significantly higher throughout the experiment (559 ± 71
47
48
49
50
51
52
53
54
55
56
57
58
59
60

1
2
3 pg/(cell/day) for the 3D scaffolds in static conditions with respect to 1248 ± 71 pg/(cell/day) for the
4
5 3D scaffolds in dynamic conditions $p < 0.00001$, ANCOVA).

6
7 We also monitored the macroscopic morphology of the cells on the 3D scaffolds and 2D films
8
9 (Figure 10). Although we found little difference between cell morphology and spreading on
10
11 scaffolds in the dynamic and static cultures, the cells grown for 5 days on 2 and 3D surfaces were
12
13 quite different. On the films cells were spread evenly and typically had larger dimensions than on
14
15 the 3D substrates, and even after 5 days, free spaces between cells were apparent. This indicates
16
17 greater cell-substrate interaction than cell-cell contact on the films. Cultures grown on 3D scaffolds
18
19 spread and migrated into the structure so that even the voids were colonised. The cells were closely
20
21 packed, and smaller, forming aggregates. This is indicative of greater interactions between adjacent
22
23 cells. Therefore even though the quantity of solid substrate is minimal, the cells seeded on the 3D
24
25 scaffolds assemble in the pores to maximize cell-cell interaction and cell density.

26 27 4 Discussion

28 Hepatocytes, like all cells, are dramatically affected by the physical and chemical nature of their
29
30 micro-environment. This is one of the reasons why *in-vitro* cell culture experiments are so difficult
31
32 to compare from laboratory to laboratory. The hepatic cell habitat comprises 3 main features, or
33
34 cues, which are known to influence cell behaviour; the biochemistry, the architecture and the supply
35
36 of nutrients to meet the metabolic demands of the cells. In this work we investigate 2 of the main
37
38 cues which are known to influence hepatocyte function, a 3D topology and convective flow.
39
40 Several investigators have shown that cell culture in 3D represents a more physiologically relevant
41
42 environment. However the extent to which this influences hepatocyte function with respect to the
43
44 provision of oxygen and other nutrients is unclear. Moreover, the relationship between the
45
46 topological features of a scaffold and hepatic function has not been studied in depth. As far as
47
48 HepG2 cells are concerned, our results show that the main contribution of the scaffold is to increase
49
50 cell density and to promote the formation of aggregates which allow greater cell-cell contact with
51
52 respect to cell-substrate interactions. Thus, we observe a large increase in the number of cells per
53
54 unit area, but the expression of albumin per cell is the same as on a monolayer, as is the glucose
55
56 consumption rate per cell, while the urea production rates also converge to similar values after 5
57
58 days in culture. Similar results have also been reported by Glicklis R *et al.* [30] and Bokhari *et al.*
59
60 [31].

On the other hand, convective transport is often mandatory in 3D scaffolds, especially if they are
thicker than a few hundred microns. Indeed, bioreactors for hepatocyte culture are generally

1
2
3 designed for allowing adequate mass transfer to high density 3 dimensional cultures in porous
4 sponges or encapsulated spheroids. One of the main engineering issues in bioreactors for *in-vitro*
5 liver models is the balance between high mass transfer and low wall shear stress to cells. There
6 appears to be some debate on the effects of shear stress on hepatocytes. Some papers cite extremely
7 high values of shear (0.5 Pa [32]) and some also report on enhancement of cytochrome expression
8 in conditions of fairly high shear stress [33]. Other investigators cite somewhat lower values of
9 maximum shear stress that these cells can support, even in the presence of non-parenchymal cells
10 which afford support and protection (0.03 Pa [34]). The application of direct fluid flow parallel to
11 the cell surface is certainly not physiological, since hepatocytes are not in direct contact with
12 flowing blood in capillaries. In this context, Wang and Tarbell's model [35] is often cited to justify
13 direct shear stress on cells of the order of 0.1 Pa [9]. These values should be applied with caution as
14 some models predict even lower values of wall shear from porous flow [36]. Here, we effectively
15 shield the cells from the effect of direct flow, although the highly permeable alginate coating allows
16 low velocity porous or percolative flow perpendicular to the convective flow provided by the
17 pumps. This flow is similar to interstitial flow [7], and allows the passage of essential nutrients and
18 catabolites thanks to concentration gradients established between the scaffold and the moving fluid.
19 In the bioreactor then, the cell density on 3D scaffolds remains unchanged with respect to static
20 cultures, but the metabolic and synthetic function in the form of albumin and urea production rates
21 per cell are greatly enhanced, as reported in Figures 6 to 9. Similar results have also been reported
22 for 2D cultures in dynamic and static conditions [28, 37] suggesting that these observations can also
23 be generalized to 2D systems.

24
25
26
27
28
29
30
31
32
33
34
35
36
37
38
39
40
41
42
43
44
45
46
47
48
49
50
51
52
53
54
55
56
57
58
59
60
The objective of this work was to recreate a biomimetic environment for hepatocytes and to
determine, first singly and then together, the influence of a 3 dimensional porous architecture and
enhanced mass transport on liver cultures. HepG2 cells were initially studied on 2D polymeric
membranes and 3D scaffolds. The results of this first stage demonstrated that the 3D scaffolds
promote cell proliferation, such that final cell densities are significantly higher than on 2D surfaces.
Other metabolic parameters were unchanged, indicating that the baseline metabolic cell function
was unaltered. While the endogenous synthetic and metabolic functions (glucose consumption rate,
albumin and urea production rates) of hepatocytes do not appear to be significantly related to cell
morphology and 3D organization, this does not necessarily mean that all functions are unaltered in
3D. In fact, Bokhari *et al.* [31] observe an increase in exogenous metabolic function in HepG2 cells
on 3D scaffolds with respect to 2D cultures, while the endogenous functions are unaltered. In the
second phase of experiments the scaffolds were placed a bioreactor and culture medium was

1
2
3 pumped through the system in a closed-loop. Neither cell proliferation nor glucose consumption
4 rate per cell increased significantly with respect to the scaffolds in static conditions, but protein
5 synthesis rates increased dramatically about 4 to 10 fold, and urea production rates by 5 to 2 fold.
6
7 These experiments established then that 3D HepG2 cultures in a dynamic environment are
8 metabolically more efficient than static monolayer hepatocyte cultures and that **the critical factor**
9 **which drives endogenous metabolism in our experiments is the interstitial-like flow.**

10
11
12 Our results demonstrate that, in order to more closely approximate functional hepatic tissue, it is
13 important to give to cells two important stimuli, the topographical and the physical stimulus. The
14 micro-topology and porosity of the three-dimensional scaffolds increases cell density due to the
15 formation of cell/cell aggregates, thus maximizing cell-cell interactions. The second stimulus is
16 produced by the flow of culture medium in the bioreactor which contributes to an increased
17 metabolic turnover. Although the hepatocytes are protected from direct open channel flow by a thin
18 coating of gel, the flow allows a sustainable supply of nutrients to the cells, as well as a physical
19 stimulus in the form of indirect interstitial-like flow.
20
21
22
23
24
25
26
27
28
29
30
31
32

33 Legends

34
35 **Figure 1: A) CAD design of one layer of the hexagonal scaffold showing approximate total**
36 **dimensions which define the nominal area. On the right, the terms unit side length and line width**
37 **are defined for one unit hexagon, B) optical micrograph of a 3D PLGA scaffold.**

38
39
40
41
42 **Figure 2: A) A three dimensional representation of the MCmB cell culture chamber, B) velocity**
43 **streamlines at a flow rate of 250 $\mu\text{l}/\text{min}$.**

44
45
46
47 Figure 3: Cell density (defined as cell number/ nominal surface area in cm^2) for 2D PLGA and
48 PLLA films, 3D PLGA and PLLA scaffolds (n=3 per data point).

49
50
51
52 Figure 4: Glucose consumption rate in static conditions in 2D films and 3D scaffolds of PLGA and
53 PLLA, (n=3 per data point).

54
55
56
57 Figure 5: Albumin production rate in static conditions for 2D films and 3D scaffolds of PLGA and
58 PLLA (n=3 per data point).
59
60

1
2
3
4
5 Figure 6: Cell density (defined as cell number/ nominal surface area in cm²) for PLGA scaffolds in
6 the bioreactor and in static conditions (n=3 per data point).
7
8
9

10 Figure 7: Glucose production rate in static and dynamic conditions for PLGA 3D scaffolds (n=3 per
11 data point).
12
13
14

15 Figure 8: Albumin production rate in static and dynamic conditions for PLGA 3D scaffolds (n=3
16 per data point).
17
18
19

20
21 Figure 9: Urea production rate in static conditions for PLGA 2D films and 3D scaffolds and in
22 dynamic conditions for PLGA 3D scaffolds (n=3 per data point).
23
24
25

26 Figure 10: Micrographs of HepG2 cells on A) PLGA film B) 3D PLGA scaffold after 5 days in
27 culture. The bar indicates 50 μm.
28
29
30

31 5. References

- 32
33 [1] Guillouzo A., Liver Cell Models in in-vitro Toxicology. *Environmental Health Perspectives*,
34 1998, 106, 551-532.
35
36 [2] Ahluwalia A., Minieri M., Dinardo P., Engineering the Stem Cell Niche: Technologies and
37 Tools for Applying Biochemical, Physical and Structural Stimuli and their effects on Stem Cells in:
38 *Stem Cell Engineering Volume 1: Principles*, Artmann G.M., Jürgen H., Minger S. (Eds), Springer-
39 Verlag, 2009, in press.
40
41 [3] Pichard-Garcia L., Gerbal-Chaloin S., Ferrini J., Fabre J. *et al.*, Use of long-term cultures of
42 human hepatocytes to study cytochrome P450 gene expression. *Methods Enzymol* 2002. 357 :311-
43 21.
44
45 [4] Harada K., Mitaka T., Miyamoto S., Sugimoto S *et al.*, Rapid formation of hepatic organoid in
46 collagen sponge by rat small hepatocytes and hepatic nonparenchymal cells. *Journal of Hepatology*,
47 2003, 39, 716-723.
48
49 [5] Chen J., Yu S., Hsu B.R., Fu S.H., Loofa Sponge as a Scaffold For the Culture Of Human
50 Hepatocyte Cell Line. *Biotechnol. Prog.* 2003, 19, 522-527.
51
52 [6] Underhill G.H., Chen A.A., Albrecht D.R., Bhatia S.N., Assessment of hepatocellular function
53 within PEG hydrogels. *Biomaterials* , 2007, 28, 256-270.
54
55
56
57
58
59
60

1
2
3
4
5
6
7
8
9
10
11
12
13
14
15
16
17
18
19
20
21
22
23
24
25
26
27
28
29
30
31
32
33
34
35
36
37
38
39
40
41
42
43
44
45
46
47
48
49
50
51
52
53
54
55
56
57
58
59
60

- [7] Rutkowski J.M., Swartz M.A., A driving force for change: interstitial flow as a morphoregulator, 2006. *TRENDS in Cell Biology* , 2006, 17, 45-50.
- [8] Catapano G., De Bartolo L., The importance of the kinetic characterization of liver cell metabolic reactions to the design of hybrid liver support devices. *Int J of Artif Organs* 1996; 19, 670-676.
- [9] Powers M.J., Domandsky K., Kaazempur-Mofrad M.R., Kalezi A. *et al.*, A microfabricated array bioreactor for perfused 3D liver culture. *Biotechnol Bioeng* 2002; 78,257-269.
- [10] Powers M.J., Janigian D., Baker C., Wack K. *et al.*, Functional behavior of primary rat liver cells in a 3D perfused microarray bioreactor. *Tissue Eng*, 2002; 8:499- 513.
- [11] Hongo T., Kajikawa M., Ishida S., Ozawa S. *et al.*, Three-Dimensional High-Density Culture of HepG2 Cells in a 5-ml Radial-Flow Bioreactor for Construction of Artificial Liver . *J. Biosci. Bioeng*, 2005, 99, 237-244.
- [12] Kataoka K., Nagao Y., Nukui T., Akiyama I. *et al.*, An organic-inorganic hybrid scaffold for the culture of HepG2 in a bioreactor. *Biomaterials*, 2005, 26 2509-2516.
- [13] Bhatia S., Yarmush M., Toner M., Controlling cell interactions by micropatterning in co-cultures: hepatocytes and 3T3 fibroblasts. *J. Biomed. Mater. Res.*, 1997, 34, 189–199.
- [14] Khetani S.R., Szulgit G., Del Rio J.A., Barlow C. *et al.*, Exploring interactions between rat hepatocytes and nonparenchymal cells using gene expression profiling. *Hepatology*, 2004, 40, 545-54.
- [15] Park J., Berthiaume F., Toner M., Yarmush M.L. *et al.*, Microfabricated grooved substrates as platforms for bioartificial liver reactors. *Biotechnol Bioeng*. 2005 , 90, 632-44.
- [16] Park J., Li Y., Berthiaume F., Toner M. *et al.*, Radial flow hepatocyte bioreactor using stacked microfabricated grooved substrates. *Biotechnol Bioeng*. 2008 99, 455-67.
- [17] Berthiaume F., Moghe P.V., Toner M., Yarmush M.L., Effect of extracellular matrix topology on cell structure, function, and physiological responsiveness: hepatocytes cultured in a sandwich configuration. *FASEB Journal.*, 1996, 10, 1471-1484.
- [18] Mazzei D., Guzzardi M. A, Giusti S., Ahluwalia A., A low shear stress modular bioreactor for connected cell culture under high flow rates. *Biotech. Bioeng (submitted)*.
- [19] Vozzi G., Previti A., De Rossi D., Ahluwalia A.. Microsyringe-based deposition of two-dimensional and three-dimensional polymer scaffolds with a well-defined geometry for application to tissue engineering. *Tissue Eng*. 2002, 8, 1089-98.

- 1
2
3 [20] Vozzi G., Ahluwalia A., Rapid Prototyping for tissue engineering applications, in: Chu P.K.,
4 Liu X.,(Eds.) *Biomaterials Fabrication and Processing Handbook*, Boca Ration, FL, CRC Press,
5 2008, 95-114.
6
7
8 [21] Mariani M., Rosatini F., Vozzi G., Previti A. *et al.*, Characterisation of Tissue Engineering
9 scaffolds microfabricated with PAM. *Tissue Engineering*, 2006, 12 , 547-558.
10
11 [22] Bhunchet E., Wake K., The portal lobule in rat liver fibrosis: a re-evaluation of the liver unit.
12 *Hepatology*. 1998, 27, 481-487.
13
14 [23] Mazzei D., Vozzi F., Cisternino A., Vozzi G. *et al.*, A high-throughput bioreactor system for
15 simulating physiological environments. *IEEE Transactions on Industrial Electronics*. 2008, 55,
16 3273-3280.
17
18 [24] Bouma M.E., Rogier E., Verthier N., Labarre C. *et al.*, Further cellular investigation of the
19 Human Hepatoblastoma- derived cell line HepG2: morphology and immunocytochemical studies of
20 Hepatic-secreted proteins. *In-vitro Cellular and Developmental Biology*. 1989,25 :267-275. [
21
22 [25] Oyaas J., Storrø I., Svendsen H., Levine D.W., The effective diffusion coefficient and the
23 distribution constant for small molecules in calcium-alginate gel beads. *Biotechnol Bioeng*. 1995,
24 47,492-500.
25
26 [26] Grassi M., Colombo I., Lapasin R., Experimental determination of the theophylline diffusion
27 coefficient in swollen sodium-alginate membranes. *J Control Release*. 2001, 76, 93-105.
28
29 [27] Venncio A., Teixeira J.A., Characterization of sugar diffusion coefficients in alginate
30 membranes. *Biotechnology Techniques*,1997, 11, 183-186.
31
32 [28] Guzzardi M.A., Vozzi F., Ahluwalia A., Study of the cross-talk between hepatocytes and
33 endothelial cells using a novel multi-compartmental bioreactor: a comparison between connected
34 cultures and co-cultures, *Tissue Eng A*. 2009. June 4, Epub.
35
36 [29] Tirella A., Orsini A., Vozzi G., Ahluwalia A., Mechanical and rheological characterization of
37 alginate for the microfabrication of geometrically controlled hydrogel scaffolds. *Bioprinting (in*
38 *press)*.
39
40 [30] Glicklis R., Shapiro L., Agbaria R. Merchuk J.C. *et al.*, Hepatocyte behavior within three-
41 dimensional porous alginate scaffolds. *Biotechnol Bioeng*. 2000, 6, 344-53.
42
43 [31] Bokhari M., Carnachan R.J., Cameron N.R., Przyborski S.A.,. Culture of HepG2 liver cells on
44 three dimensional polystyrene scaffolds enhances cell structure and function during toxicological
45 challenge. *Anat*. 2007, 211, 567–576.
46
47 [32] Tanaka Y., Yamato M., Okano T., Kitamori T. *et al.*, Evaluation of effects of shear stress on
48 hepatocytes by a microchip-based system. *Meas. Sci. Technol*. 2006, 17, 3167–3170.
49
50
51
52
53
54
55
56
57
58
59
60

- 1
2
3 [33] Mufti N.A., Shuler M.L. Induction of cytochrome P-450IA1 activity in response to sublethal
4 stresses in microcarrier-attached Hep G2 cells. *Biotechnol Prog.* 11(6):659-63, 1995
5
6 [34] Tilles A.W., Baskaran H., Roy P, Yarmush M.L. *et al.*, Effects of oxygenation and flow on the
7 viability and function of rat hepatocytes cocultured in a microchannel flat-plate bioreactor.
8
9 *Biotechnol Bioeng.* 73(5):379-89, 2001.
10
11 [35] Wang D.M., Tarbell J.M.. Modeling interstitial flow in an artery wall allows estimation of wall
12 shear stress on smooth muscle cells. *J Biomech Eng.* 1995 ,117, 358-63.
13
14 [36] Boschetti F., Raimondi M., Migliavacca F., Dubini G., Prediction of the micro-fluid dynamic
15 environment imposed to three-dimensional engineered cell systems in bioreactors. *J. Biomechanics.*
16 2006,39, 418-425.
17
18 [37] Vozzi F., Heinrich J.M., Bader A., Ahluwalia A.D., Connected culture of murine hepatocytes
19 and HUVEC in a multicompartmental bioreactor. *Tissue Eng A.* 2009 , 15, 1291-9.
20
21
22
23
24
25
26
27
28
29
30
31
32
33
34
35
36
37
38
39
40
41
42
43
44
45
46
47
48
49
50
51
52
53
54
55
56
57
58
59
60

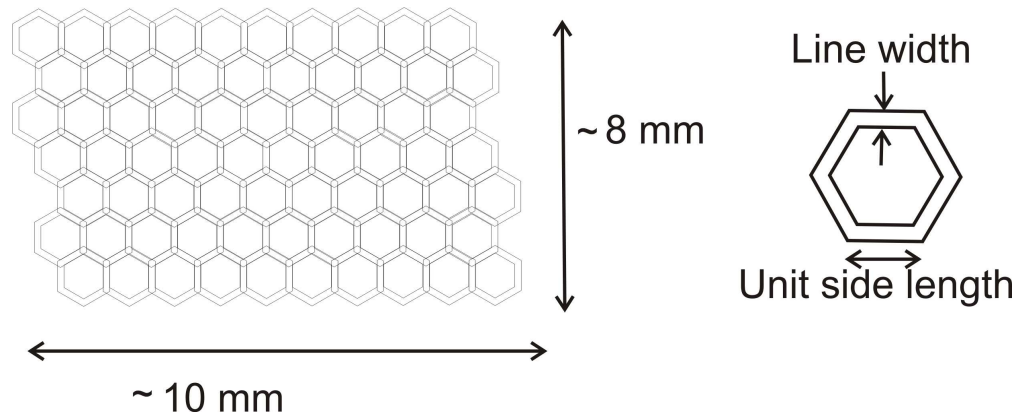


Figure 1: A) CAD design of one layer of the hexagonal scaffold showing approximate total dimensions which define the nominal area. On the right, the terms unit side length and line width are defined for one unit hexagon, B) optical micrograph of a 3D PLGA scaffold.

Peer Review

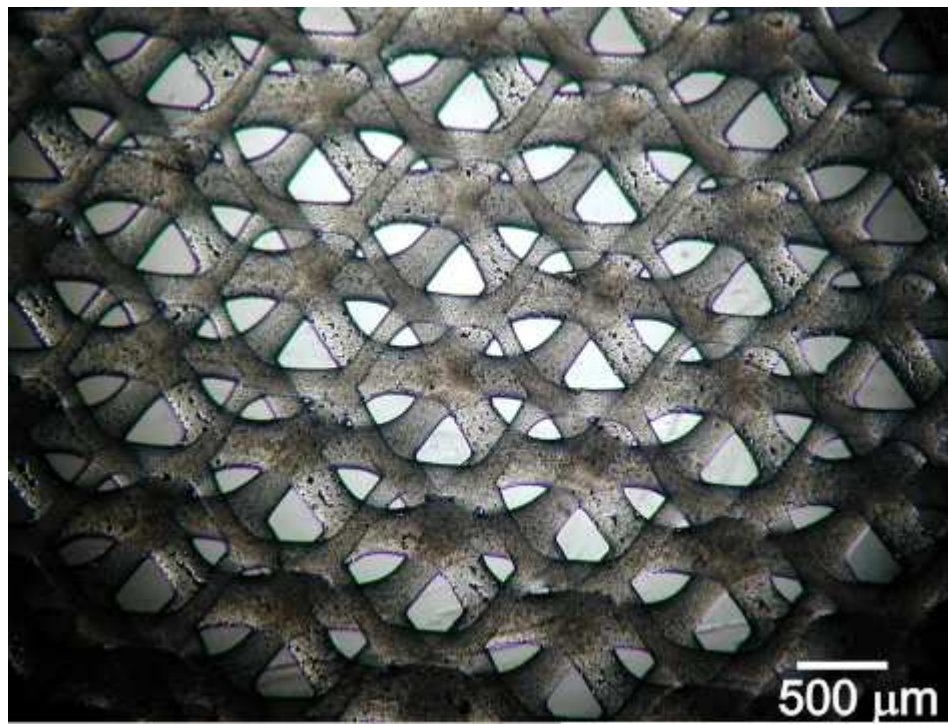


Figure 1: A) CAD design of one layer of the hexagonal scaffold showing approximate total dimensions which define the nominal area. On the right, the terms unit side length and line width are defined for one unit hexagon, B) optical micrograph of a 3D PLGA scaffold.

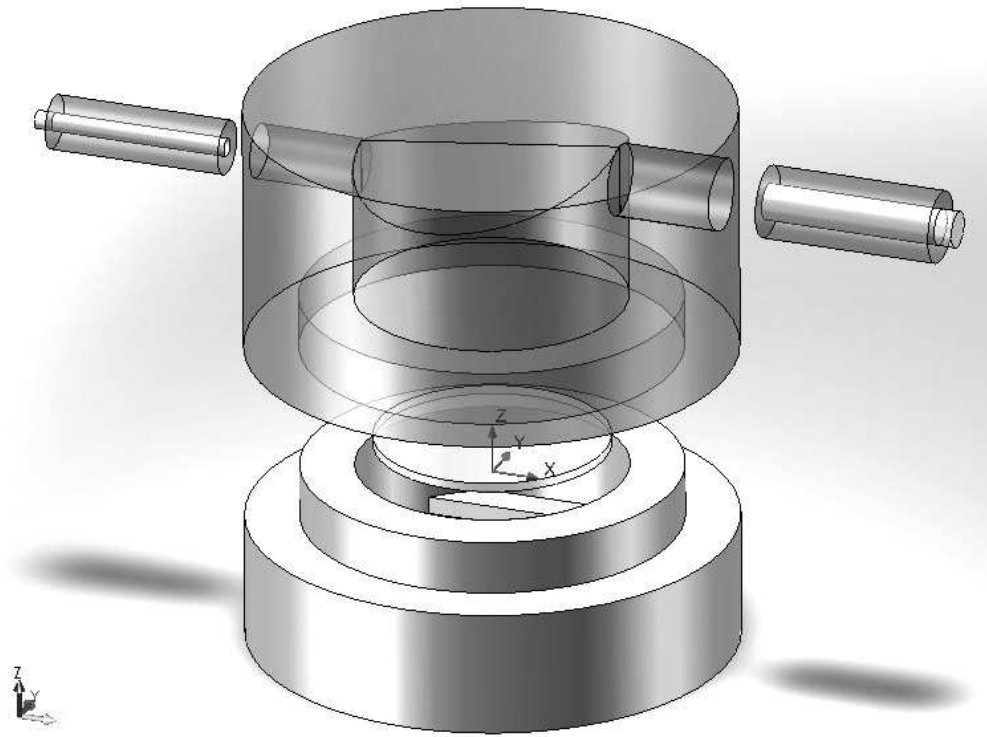


Figure 2: A) A three dimensional representation of the MCmB cell culture chamber, B) velocity streamlines at a flow rate of 250 $\mu\text{l}/\text{min}$.

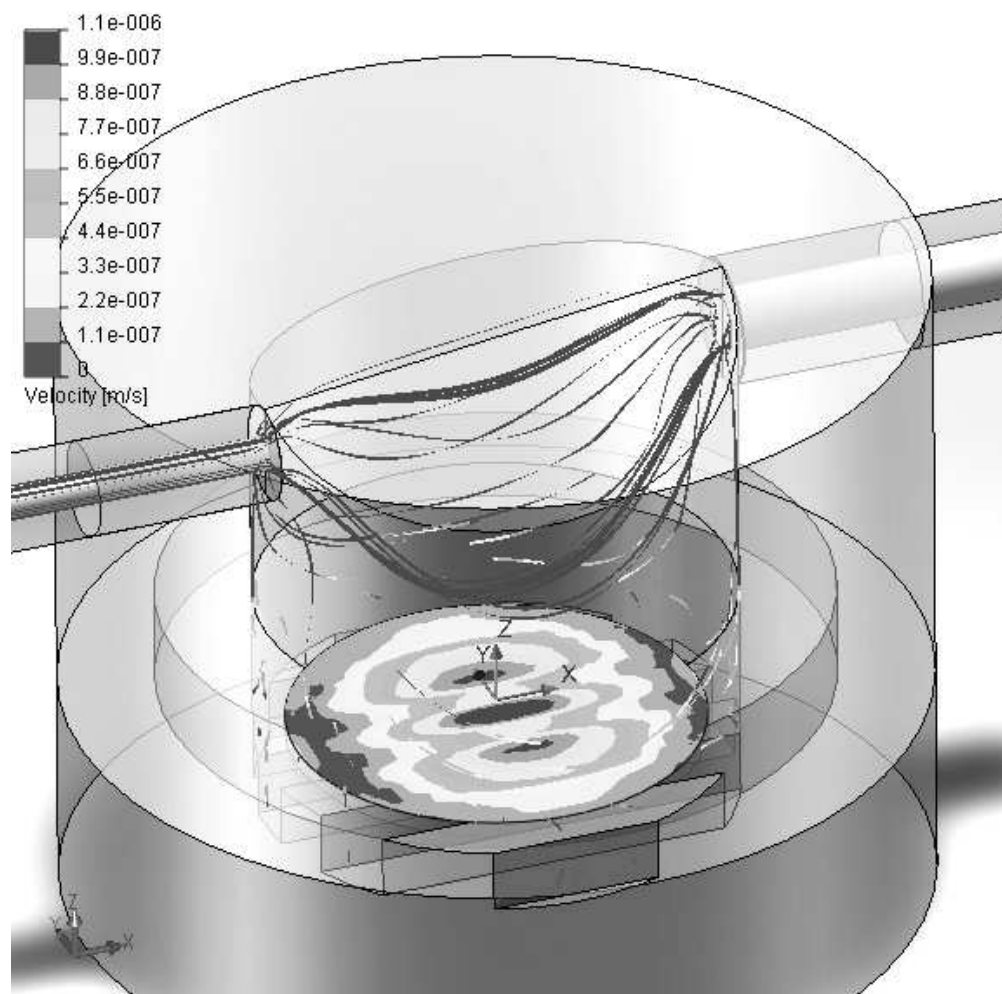


Figure 2: A) A three dimensional representation of the MCmB cell culture chamber, B) velocity streamlines at a flow rate of 250 $\mu\text{l}/\text{min}$.

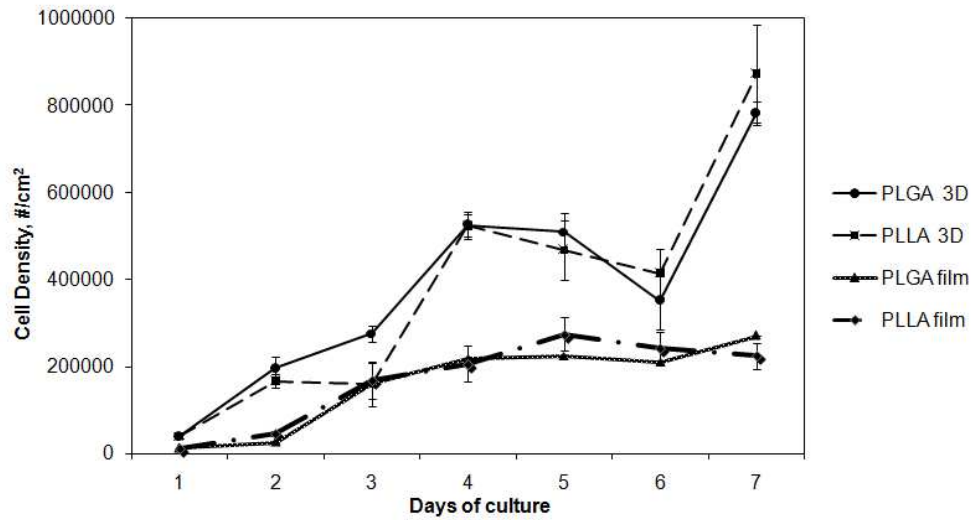


Figure 3: Cell density (defined as cell number/ nominal surface area in cm²) for 2D PLGA and PLLA films, 3D PLGA and PLLA scaffolds (n=3 per data point).

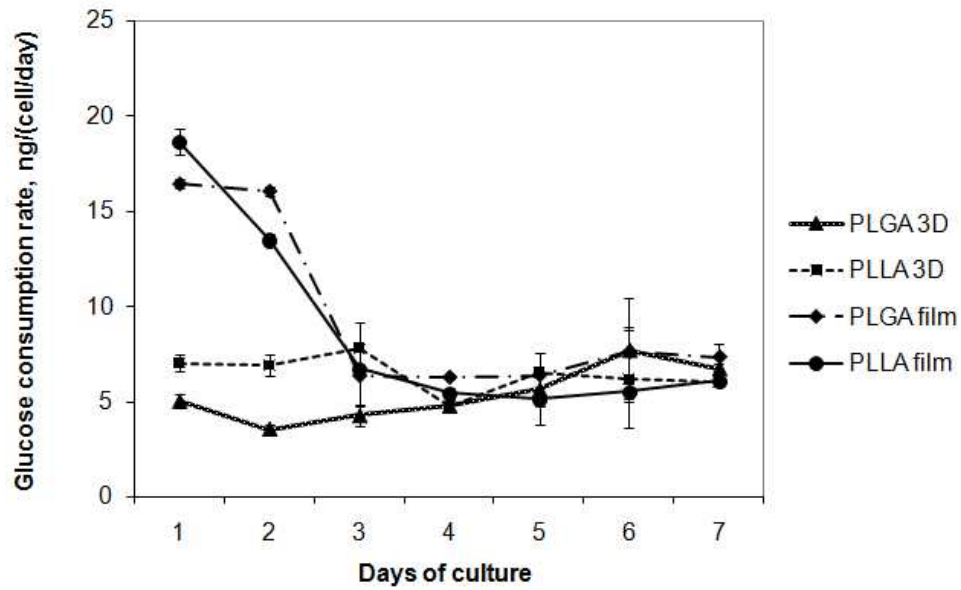


Figure 4: Glucose consumption rate in static conditions in 2D films and 3D scaffolds of PLGA and PLLA, (n=3 per data point).

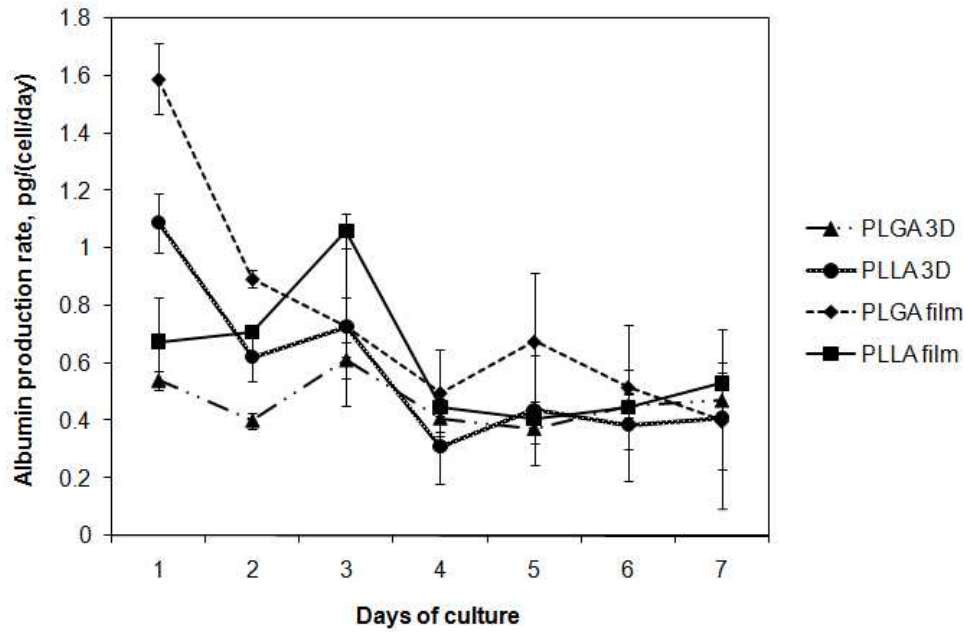


Figure 5: Albumin production rate in static conditions for 2D films and 3D scaffolds of PLGA and PLLA (n=3 per data point).

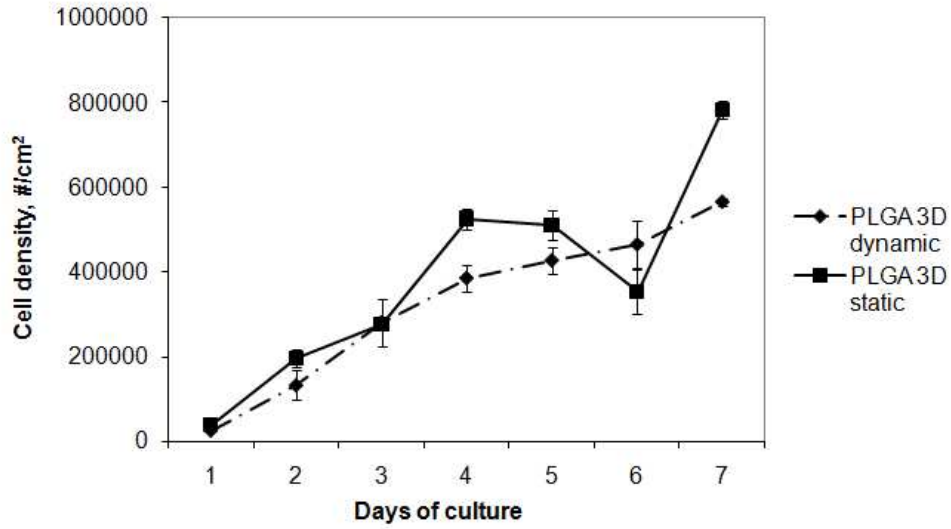


Figure 6: Cell density (defined as cell number/ nominal surface area in cm²) for PLGA scaffolds in the bioreactor and in static conditions (n=3 per data point).

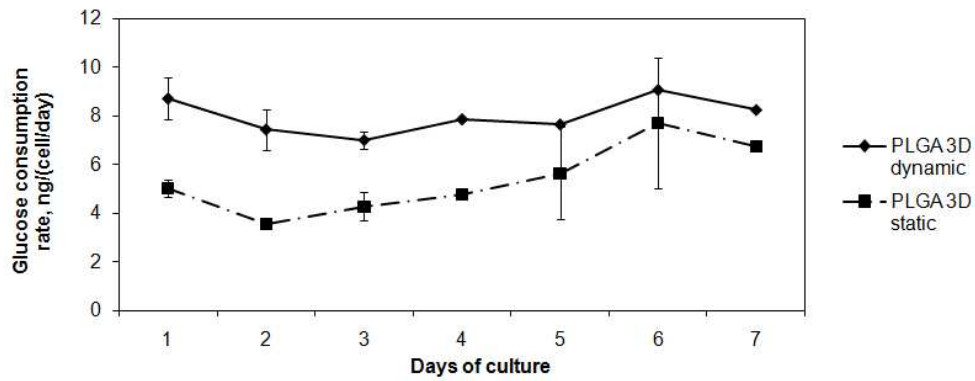


Figure 7: Glucose production rate in static and dynamic conditions for PLGA 3D scaffolds (n=3 per data point).

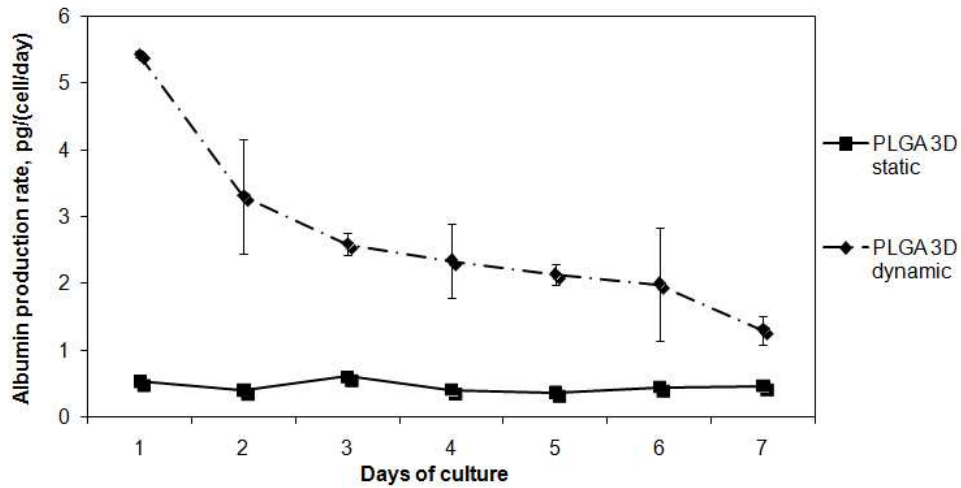


Figure 8: Albumin production rate in static and dynamic conditions for PLGA 3D scaffolds (n=3 per data point).

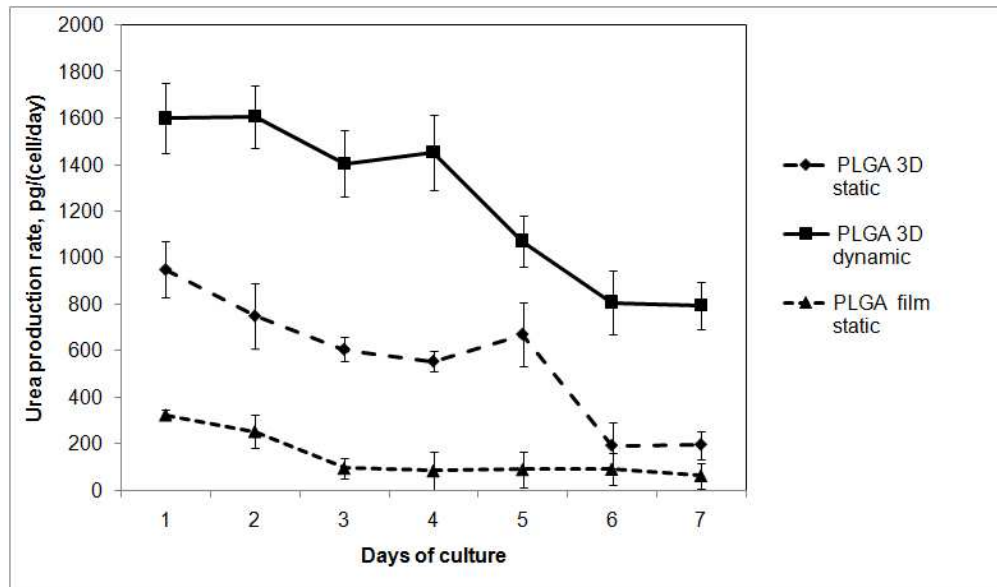
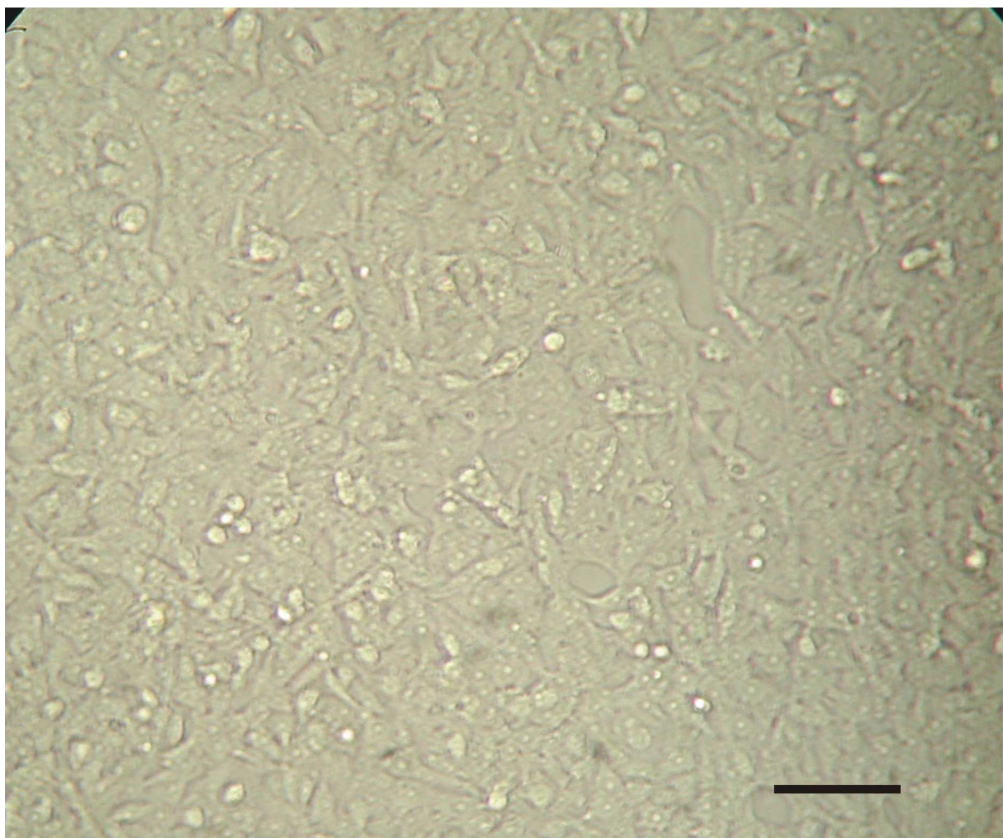


Figure 9: Urea production rate in static conditions for PLGA 2D films and 3D scaffolds and in dynamic conditions for PLGA 3D scaffolds (n=3 per data point).

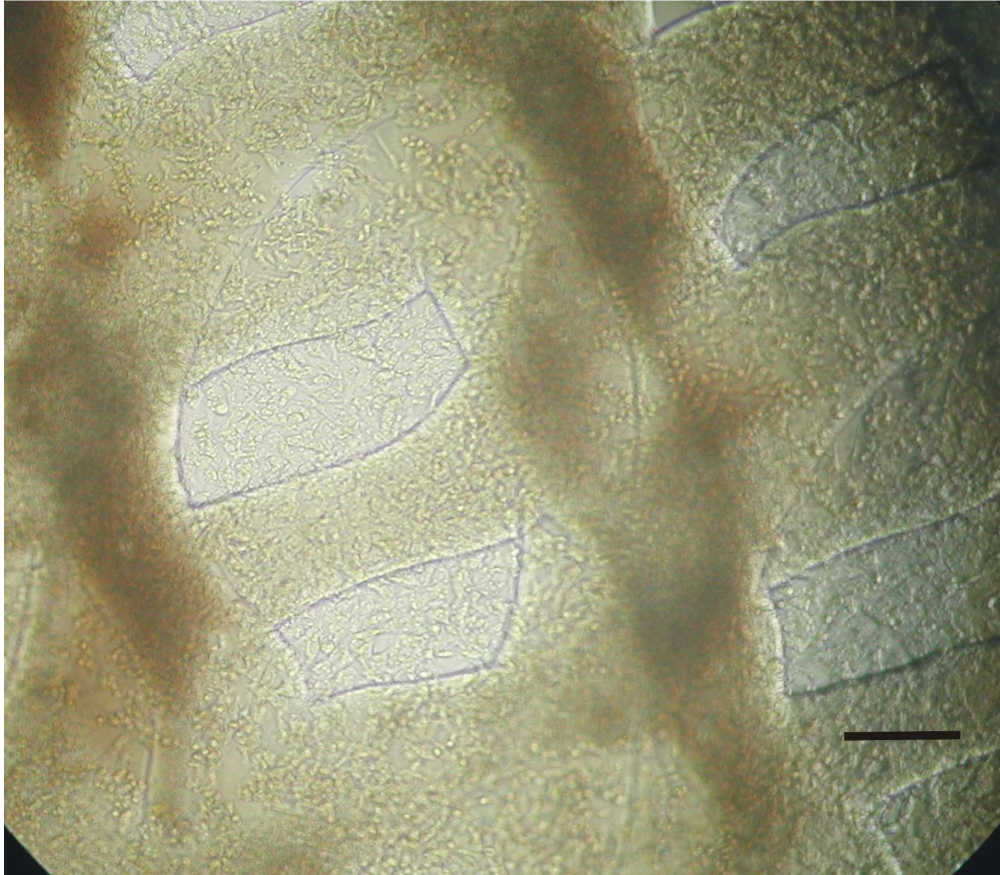
1
2
3
4
5
6
7
8
9
10
11
12
13
14
15
16
17
18
19
20
21
22
23
24
25
26
27
28
29
30
31
32
33
34
35
36
37
38
39
40
41
42
43
44
45
46
47
48
49
50
51
52
53
54
55
56
57
58
59
60



317x264mm (300 x 300 DPI)

view

1
2
3
4
5
6
7
8
9
10
11
12
13
14
15
16
17
18
19
20
21
22
23
24
25
26
27
28
29
30
31
32
33
34
35
36
37
38
39
40
41
42
43
44
45
46
47
48
49
50
51
52
53
54
55
56
57
58
59
60



317x278mm (300 x 300 DPI)